Supplementary Information for:

Increased intracellular Ca^{2+} concentrations prevent membrane localization of PH domains through the formation of Ca^{2+}-phosphoinositides

Jin Ku Kang*, Ok-Hee Kim*, June Hur*, So Hee Yu*, Santosh Lamichhane*, Jin Wook Lee*, Uttam Ojha*, Jeong Hee Hong*, Cheol Soon Lee*, Ji-Young Cha†, Young Jae Lee†, Seung-Soon lm‡, Young Joo, Park#, Cheol Soo Choi*, Dae Ho Lee*, In-Kyu Lee§, Byung-Chul Oh*¶

*Lee Gil Ya Cancer and Diabetes Institute, Gachon University, College of Medicine, Department of Physiology, 155 Gaetbeol-ro, Yeonsu-gu, Incheon, 406-840, Korea

†Lee Gil Ya Cancer and Diabetes Institute Gachon University, College of Medicine, Department of Biochemistry, 155 Gaetbeol-ro, Yeonsu-gu, Incheon, 406-840, Korea

#Department of Internal Medicine, Seoul National University College of Medicine, Seoul, Republic of Korea

‡Department of Physiology, Keimyung University School of Medicine, Daegu 704-701, South Korea

§Department of Internal Medicine, Graduate School of Medicine, Kyungpook National University, Daegu 702-701, Korea

Materials and Methods

Antibodies, cell lines, and immunoblotting.

Tissues and cells were lysed with lysis buffer (Cell Signaling Technology), and equal amounts of protein were resolved on 4–12% gels and electrophoretically transferred to polyvinylidene difluoride (PVDF) membranes. The following antibodies were used for immunoblotting, confocal microscopy, and flow cytometry: Akt (C67E7, Cell signaling), hAkt PH domain (SKB1, Millipore), pAkt T308 (C31E5E, Cell Signaling), pAkt S473 (D9E, Cell Signaling), GSK3β (HPA002127, Atlas Antibodies), pGSK S9 (D85E12, Cell signaling), FOXO3 (ab12162, Abcam), pFOXO3 S253 (ab47285, Abcam), pAS160 T642 (#4288, Cell Signaling), AS160 (#2447, Cell Signaling), β-actin (AC-15, Sigma-Aldrich), and 6x histidine tag (GT359, Sigma-Aldrich). Cell lines obtained from the American Type Culture Collection (ATCC, Manassas, VA, USA) were authenticated by short tandem repeats (HEK293T and HepG2) or interspecies analysis (CHO-IR and Raw264.7) and were mycoplasma free.

Animal care and use.

C57Bl/6 male mice from Orient Bio Inc. (Korea) were studied under protocols approved by the animal ethics committee of Gachon University, Lee Gil Ya Cancer and Diabetes Institute, (LCDI-2014-0080). Mice were maintained with a 12-h light/12-h dark cycle and provided with food and water. For diet-induced obesity studies, male mice were placed on a 60% high fat diet or a 10% control diet (catalog no. D12492 and D12450B, respectively; Research Diets) at weaning for 8 weeks. Body weight and food intake were measured weekly. Food intake was measured for each cage (three mice per cage) and divided by mouse number to obtain total grams consumed per mouse per week.

Adenovirus

GCaMP6m adenovirus (#1909) was purchased from Vector Biolabs. Akt PH-mCherry was cloned into the pAdTrack-CMV shuttle vector. Adenoviral constructs were created by recombination of the shuttle vector and the pAdEasy vector by electroporation into BJ5183-AD-1 bacteria (Stratagene). Recombinant adenovirus (5×10^8 plaque-forming

units) was delivered by systemic tail-vein injection to C57BL/6J mice fed a 60% high-fat diet or a 10% control diet for 10 weeks. After 7 days of adenoviral infection, the livers were collected from mice following overnight fasting and from those that were subsequently re-fed with normal chow or HFD for 4 h.

Measurement of intracellular Ca^{2+} concentration

HepG2 cells were plated onto slide glass and incubated with 4 μM Fura-2-AM (Teflabs) in physiological salt solution (PSS) at room temperature in the dark and then washed for 10 min with PSS. Changes in intracellular Ca^{2+} concentration were determined by measuring the fluorescence intensities using dual excitation wavelengths of 340 and 380 nm, and an emission wavelength of 510 nm. Results are presented as fluorescence (F) ratios (Ratio = F340/380). Emitted fluorescence was monitored using a CCD camera (Photometrics, AZ) attached to an inverted microscope (Olympus, Japan) and analyzed with a MetaFluor system (Molecular Devices, PA). Fluorescence images were obtained at 1-s intervals and the background fluorescence at each excitation wavelength was subtracted from the raw signal. ΔCa^{2+} responses were calculated by the difference between basal Ca^{2+} levels and the maximum Ca^{2+} peak of stimulated state with or without palmitic acid. For immunofluorescence, isolated primary mouse hepatocytes or cells were plated onto slide glass and incubated with 5 μM Fluo-3 AM (Invitrogen) for 45 min. Then cells were counterstained with 4,6-diamidino-2-phenylindole (DAPI) to visualize the nuclei. After mounting, the sections were imaged with a Zeiss LSM 700 laser-scanning confocal microscope (Carl Zeiss) and analyzed with ZEN 2010 Software (Carl Zeiss). The quantification of intracellular Ca^{2+} was analyzed using NIH ImageJ software (https://imagej.nih.gov/ij/, 1997-2017). Data are presented as fold changes.

Protein expression and phospholipid binding specificity. The cDNA encoding the hAkt PH domain (residues 1–144) was subcloned into the pmCherry-C1 vector (TaKaRa Clontech). The cDNA encoding the hPLCd PH domain was purchased from Addgene. CHO cells were transfected using Lipofectamine (Life Technologies) and selected using blasticidin. cDNAs encoding PH domains from hAkt (1–144), hPLCδ (1–174), and hIRS1 (9–156) were subcloned into the pET28a vector (Novagene);

recombinant proteins with C-terminal His_6 tags were expressed in *Escherichia coli* and purified using Ni-NTA resin and gel filtration. Immobilized phospholipids (P-6001 PIP strips and P-6100 PIP arrays, Echelon Bioscience) were used to assess the binding specificity of recombinant PH domains from Akt, PLCδ, and IRS1 as described.

Isothermal titration calorimetry (ITC)

To measure the binding isotherms for Ca^{2+} binding to PIPs or recombinant Akt PH domain, we performed isothermal titration calorimetric (ITC) experiments using a MicroCal 200 isothermal titration microcalorimeter (MicroCal), as previously described (1). Briefly, titrations entailed injecting 1–1.5 µL of 2 mM $CaCl_2$ into 0.1 mM PIPs in 10 mM HEPES, pH 7.0 at 25°C. Curves were fit using Origin Software (Microcal). Use of the appropriate model to fit the binding isotherm data provided information on the binding constant (Ka), change in enthalpy (ΔH), and stoichiometry of binding (n). The Gibbs free energy (ΔG) was calculated from the enthalpy change (ΔH) and binding constant (Ka) using the equation: $\Delta G = RTlnKa = \Delta H T\Delta S$, where R is the gas constant and T is the absolute temperature in degrees Kelvin. Liposomes were generated by mixing chloroform solutions of 1-palmitoyl-2-oleoyl-sn-glycero-3-phosphocholine (POPC) with 1-palmitolyl-2-oleoyl-sn-glycero-3-phosphoserine (POPS), 1,2-dipalmotoyl-sn-glycero-3-phosphatidylinositol-4,5-trisphosphate ($PI(3,4)P_2$), 1,2-dipalmotoyl-sn-glycero-3-phosphatidylinositol-4,5-trisphosphate ($PI(4,5)P_2$) or 1,2-dipalmotoyl-sn-glycero-3-phosphatidylinositol-3,4,5-trisphosphate ($PI(3,4,5)P_3$) (Cayman Chemicals, USA) in 80:20 molar ratios. Organic solvents were removed and phospholipids were vortexed to produce unilamellar vesicles in HEPES, pH 7.0.

Statistical analysis.

Unless otherwise noted, graphical presentations represent mean ± standard error margin (SEM). Differences between groups were examined for statistical significance using two-tailed unpaired Student's *t*-tests and $P < 0.05$ as the cut-off value. The variances between groups were similar, as their coefficients of variation were similar when calculated by Graphpad Prism software (GraphPad Software, Inc., La Jolla, CA, USA).

Reference

1. Kim OH, *et al.* (2010) beta-propeller phytase hydrolyzes insoluble Ca(2+)-phytate salts and completely abrogates the ability of phytate to chelate metal ions. *Biochemistry* 49(47):10216-10227.

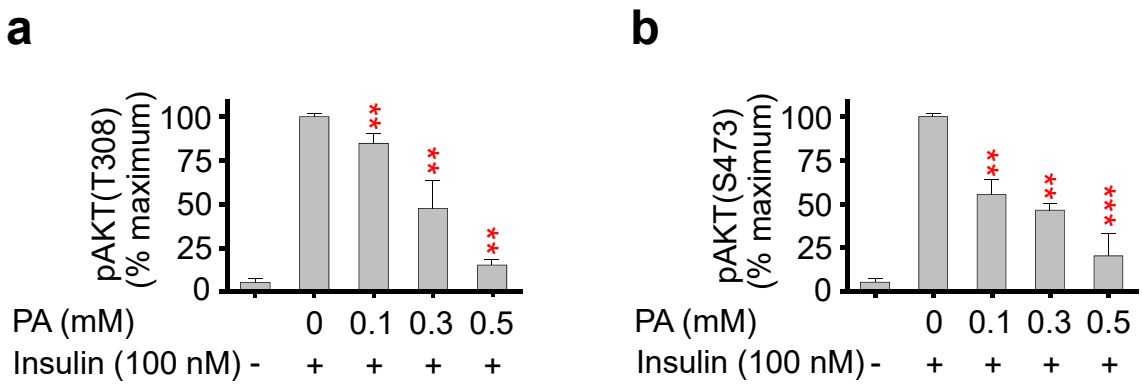

Figure S1. Quantification of Akt phosphorylation at T308 and S473 in HepG2 cells treated with increasing concentrations of palmitic acid. Quantification of Akt phosphorylation was analyzed using imageQuant LAS 4000. Data represent means ± SEM (n = 3, *P < 0.05, **P < 0.01, ***P < 0.001)

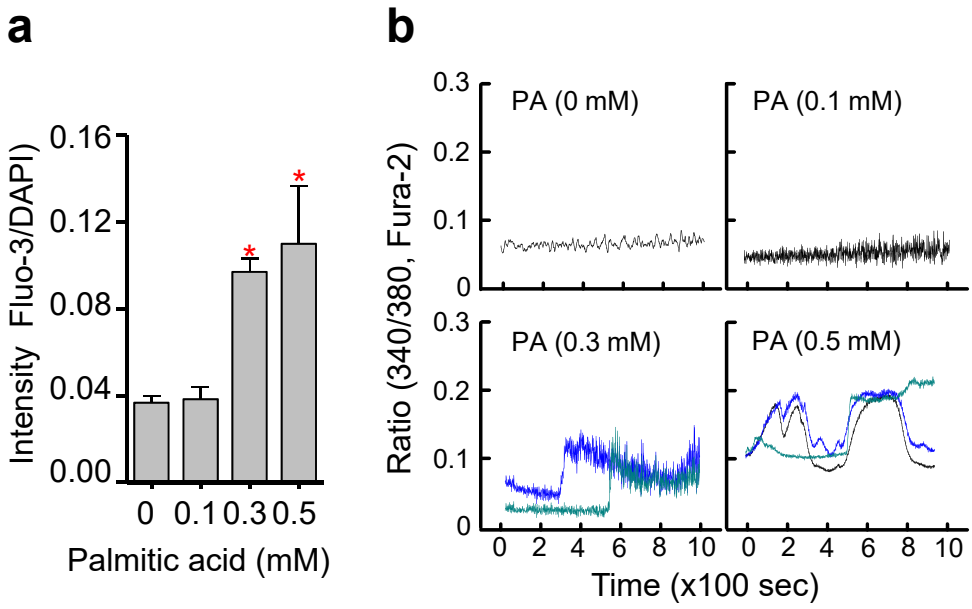

Figure S2. Palmitic acid treatment increases intracellular Ca^{2+} levels. a. Mean traces of intracellular $[Ca^{2+}]i$ dynamics in Fura-2 AM-loaded HepG2 cells pretreated with palmitic acid for the indicated time periods. Data represent means ± SEM (n = 4, **P* < 0.05). The values are presented as the ratio of fluorescence at 340 nm to that at 380 nm (340/380). Analysis of palmitic acid-induced basal and maximum $[Ca^{2+}]i$ peaks were determined using R340/380 fluorescence ratio. Data represent means ± SEM. **P* < 0.05. **b**. Mean traces for the time-dependent changes in intracellular Ca^{2+} in Fura-2-loaded HepG2 cells pretreated with the indicated concentrations of palmitic acid for 24 h.

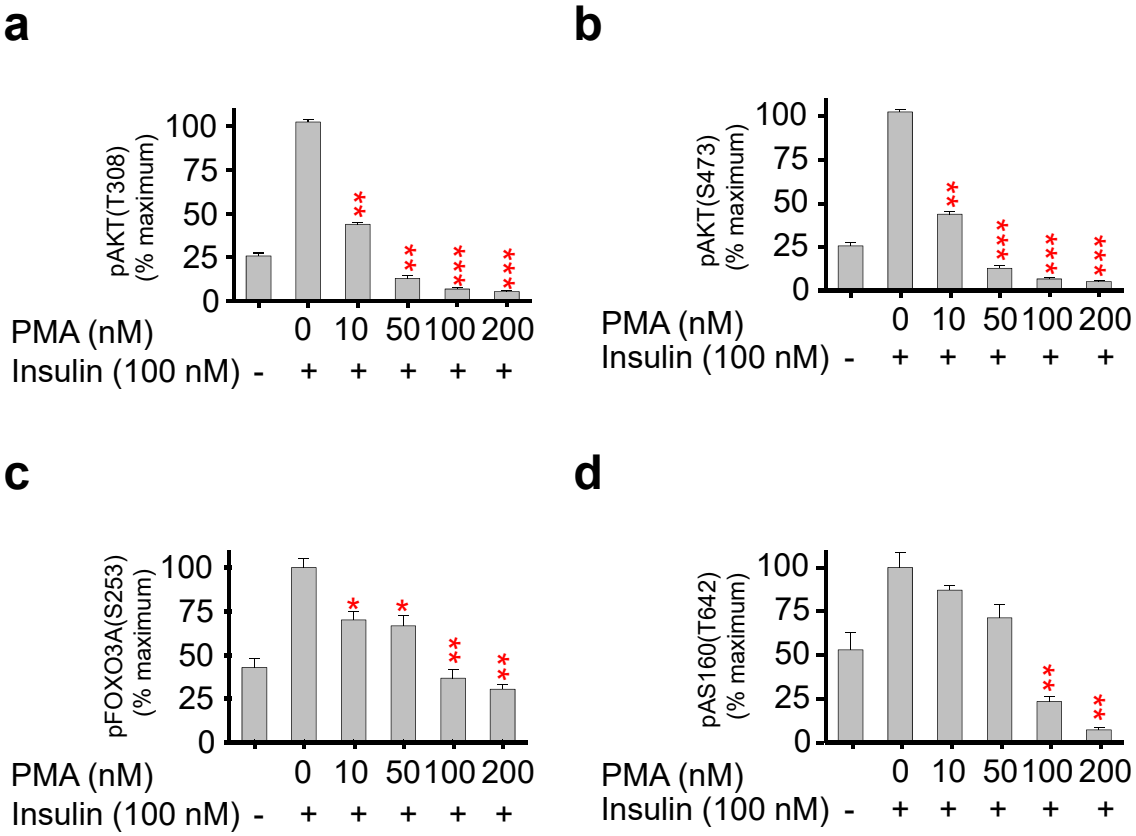

Figure S3. Quantification of the phosphorylation of Akt at T308 (**a**), S473 (**b**), FOXO3A (**c**), and AS160 (**d**) in HepG2 cells treated with increasing concentrations of PMA. Quantification of protein phosphorylation was analyzed using imageQuant LAS 4000. Data represent means ± SEM (n = 3, *P < 0.05, **P < 0.01, ***P < 0.001)

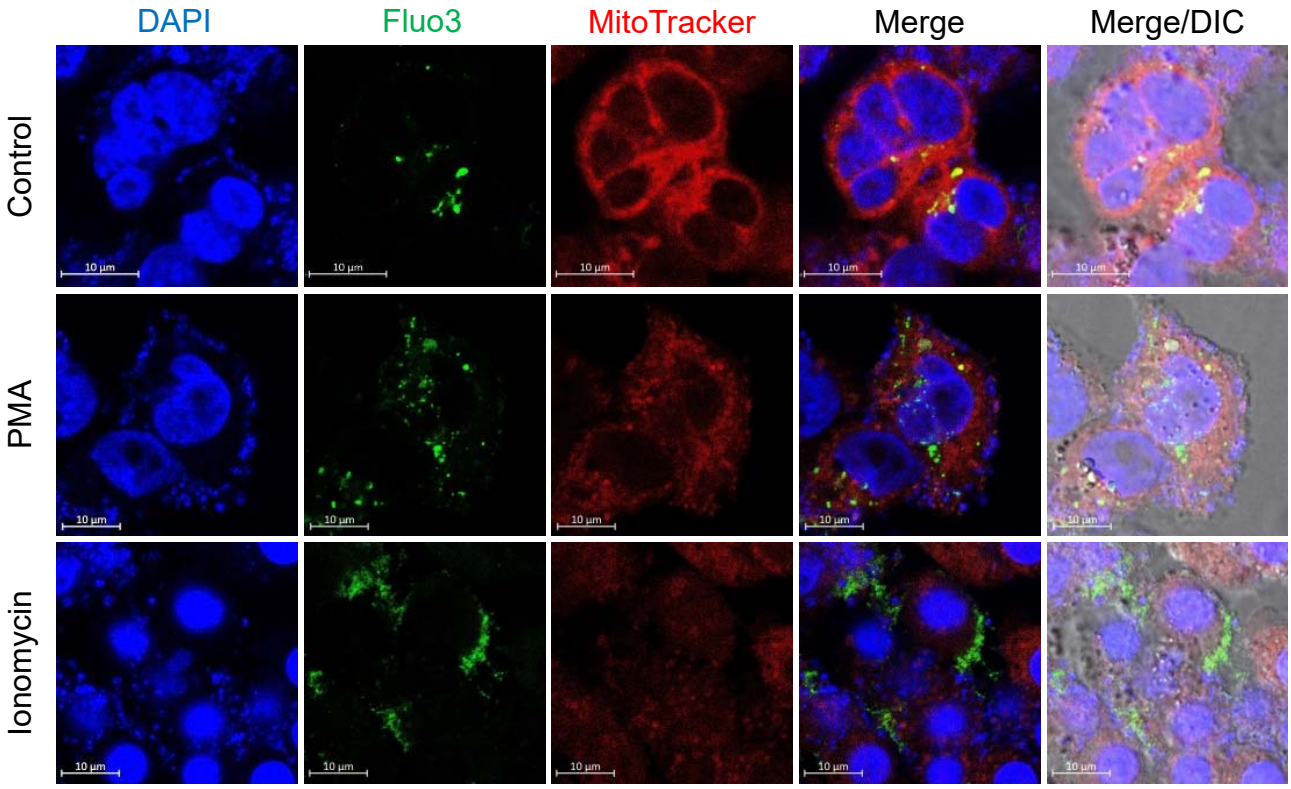

Figure S4. **Representative Fluo-3 AM images of cytosolic Ca^{2+} and MitoTracker images of mitochondria in HepG2 cells pretreated with PMA or ionomycin.** Representative Fluo-3 AM images of cytosolic Ca^{2+} and MitoTracker images of mitochondria in HepG2 cells pretreated with PMA or ionomycin. To confirm whether imaging patterns of intracellular Ca^{2+} with Fluo-3 AM differ from those of mitochondria, we compared their staining with a double-staining approach by labeling the cells with both MitoTracker and Fluo-3 AM after pretreating the HepG2 cells with PMA or ionomycin. HepG2 cells were incubated with the calcium indicator Fluo-3 AM (4 uM) and MitoTracker red (500 nM) for 45 min and the images were visualized using confocal microscopy (scale bar = 10 μM). Confocal images show Fluo-3 AM localized to the cytoplasm as a punctate distribution but not overlapping significantly with the mitochondria. Imaging of intracellular Ca^{2+} stains with Fluo-3 AM showed a punctate distribution, distinct from that of mitochondria in HepG2 cells (Fig. S5), indicating that the images with Fluo-3 AM may reflect intracellular free Ca^{2+}.

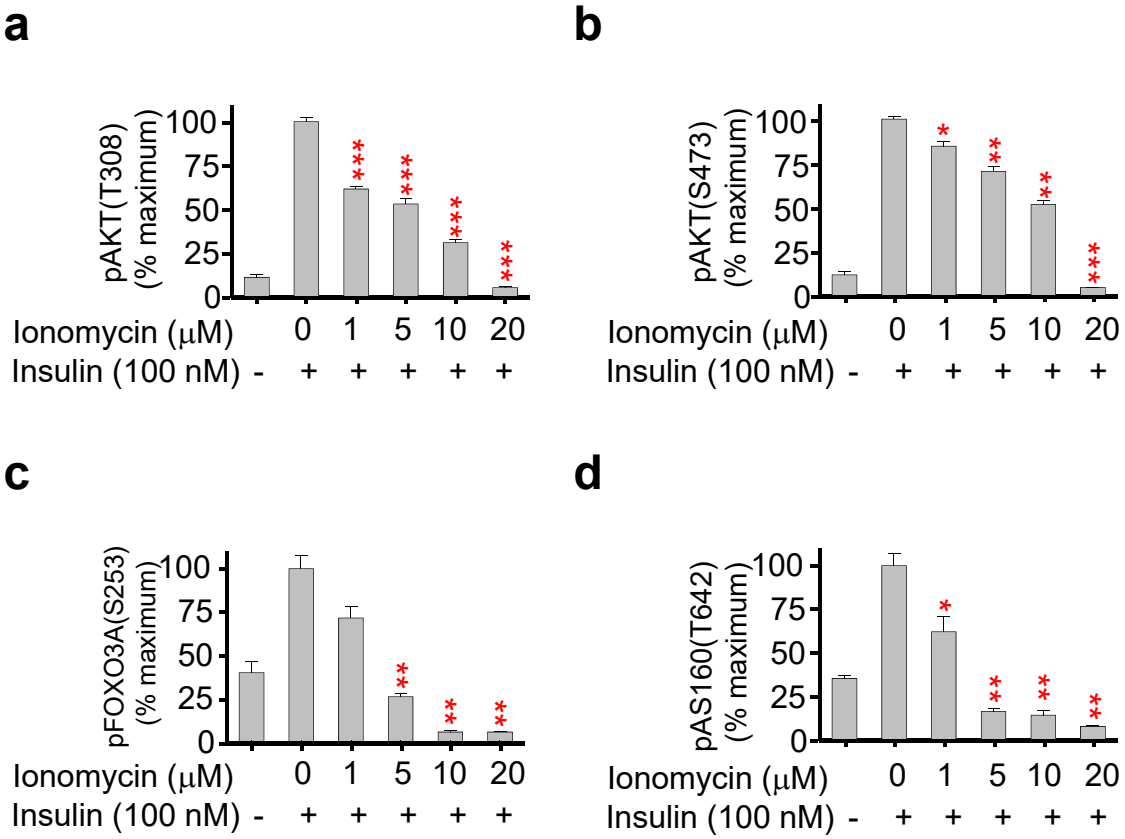

Figure S5. **The effects of ionomycin on insulin-stimulated phosphorylation of Akt**. Quantification of phosphorylation of Akt at T308 (a), S473 (b), FOXO3A (c), and AS160 (d) in HepG2 cells treated with increasing concentration of ionomycin. Quantification of protein phosphorylation was analyzed using imageQuant LAS 4000. Data represent means ± SEM (n = 3, *P < 0.05, **P < 0.01, ***P < 0.001)

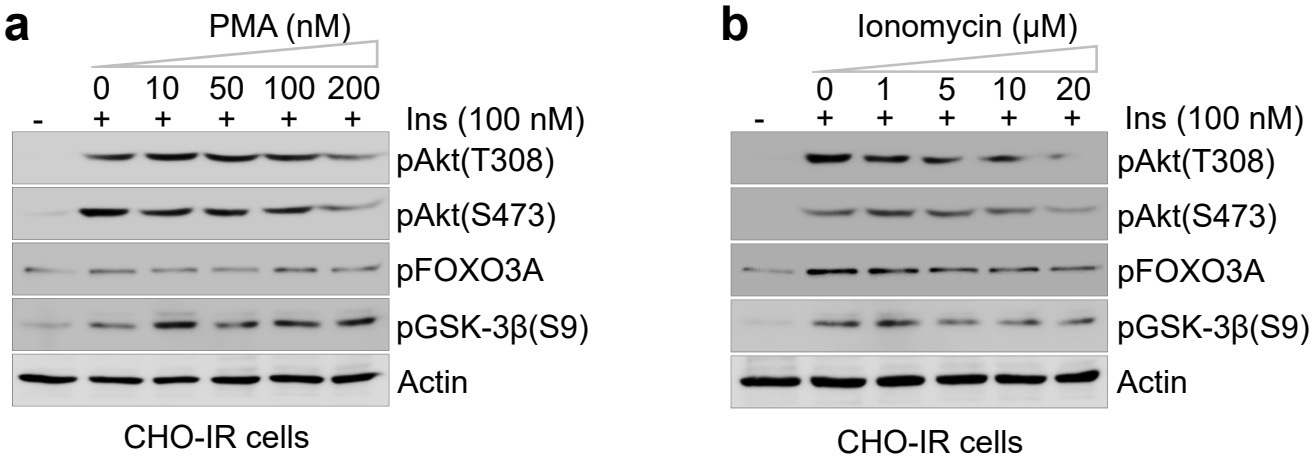

Figure S6. **The catalytic activity of Akt is modulated by the intracellular Ca^{2+} concentration**. **a**,**b**. Immunoblot analysis of phosphorylation states of Akt and total amounts of the indicated proteins in CHO-IR cells. Cells were incubated for 30 min with various concentrations of PMA (**a**) or ionomycin (**b**), followed by treatment with 100 nM insulin for 15 min.

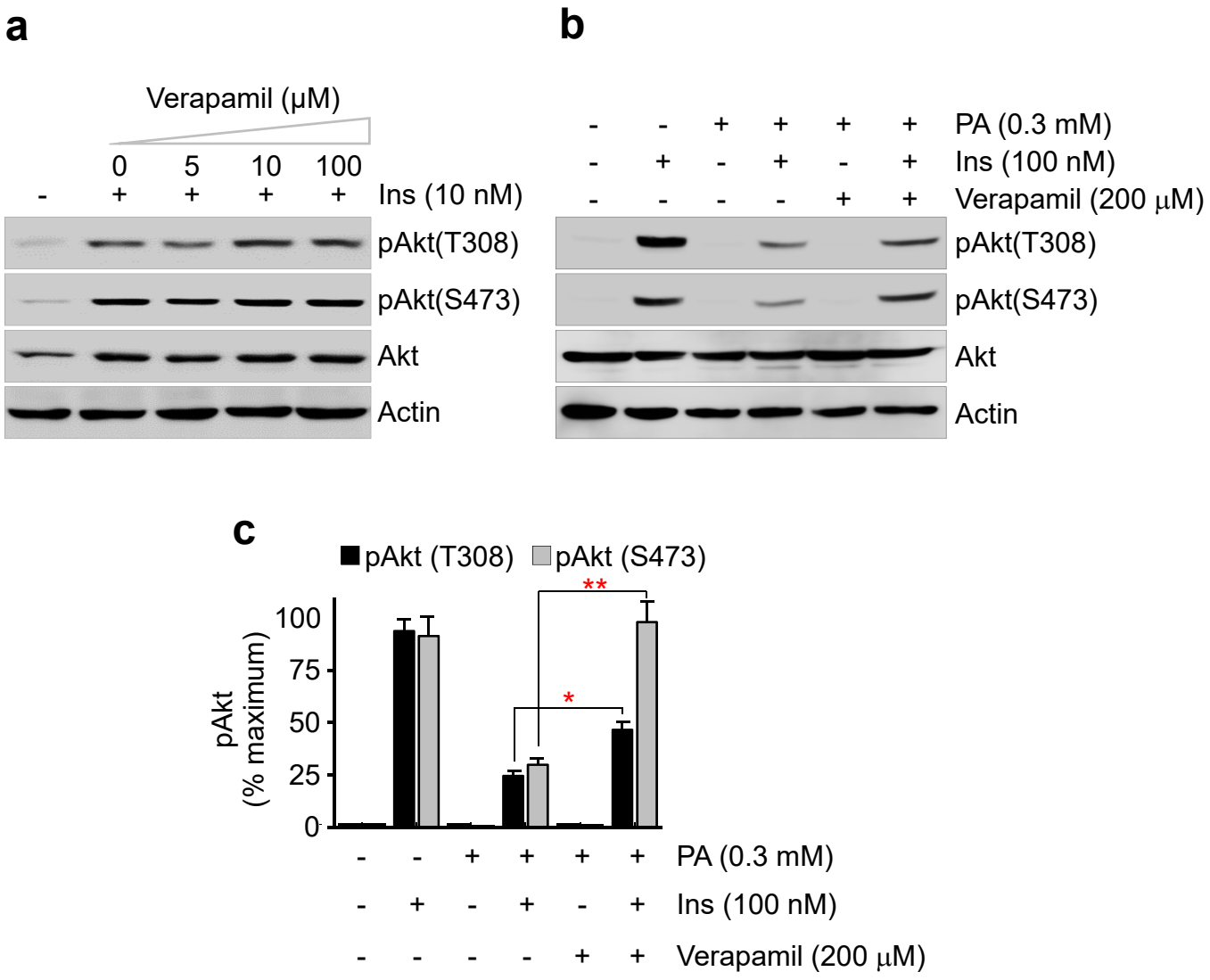

Figure S7. **The effects of verapamil on Akt phosphorylation in HepG2 cells. a**. Immunoblot analysis of the phosphorylation states of Akt and the total amounts of the indicated proteins in HepG2 cells. Cells were incubated for 1 h with the indicated concentrations of verapamil, followed by treatment with 10 nM insulin for 15 min. **b**. Immunoblot analysis of the phosphorylation states and the total amounts of Akt in HepG2 cells. After a 24 h pretreatment of HepG2 cells with 0.3 mM palmitic acid, cells were incubated for 6 h with 200 nM of verapamil, followed by treatment with 100 nM insulin for 15 min. **c**. After pretreating HepG2 cells with 0.3 mM palmitic acid for 24 h, cells were incubated for 6 h with 200 nM of verapamil, followed by treatment with 100 nM insulin for 15 min. Quantification of Akt phosphorylation was analyzed using imageQuant LAS 4000. Data represent means ± SEM (n = 3, *P < 0.05, **P < 0.01)

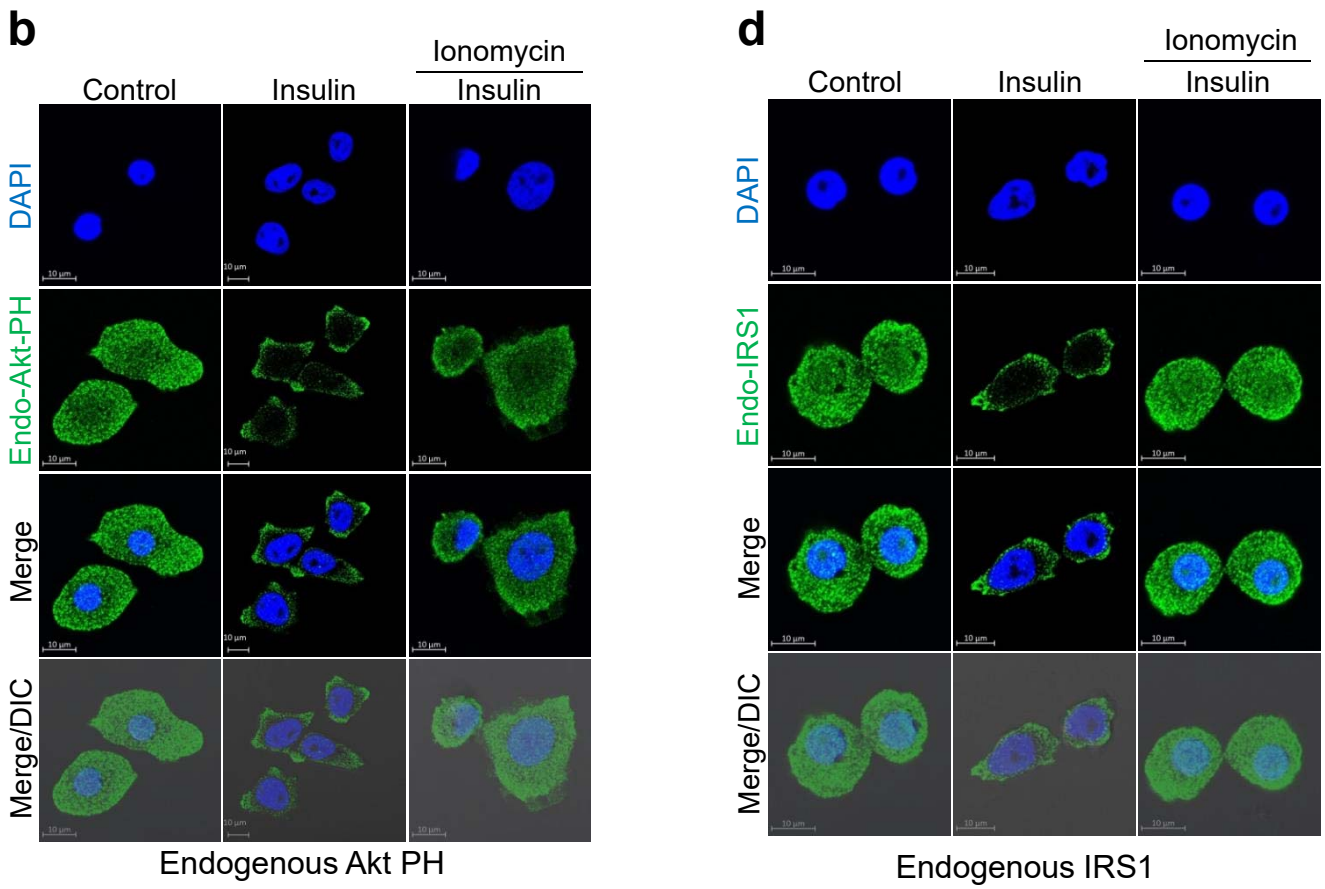

Figure S8. Higher intracellular Ca^{2+} concentrations prevent membrane localization of PH domain proteins. a. Representative fluorescence images of endogenous Akt in CHO-IR cells. CHO-IR cells were serum-starved for 3 h, followed by pretreatment with or without ionomycin for 30 min before a 15-min stimulation with 100 nM insulin. Cells were stained with anti-Akt PH domain antibody and visualized with FITC-conjugated secondary antibody. **b**. Representative fluorescence images of endogenous IRS1 in CHO-IR cells. CHO-IR cells were serum-starved for 3 h, followed by pretreatment with or without ionomycin for 30 min before a 15-min stimulation with 100 nM insulin. Cells were stained with anti-IRS1 antibody and visualized with FITC-conjugated secondary antibody.

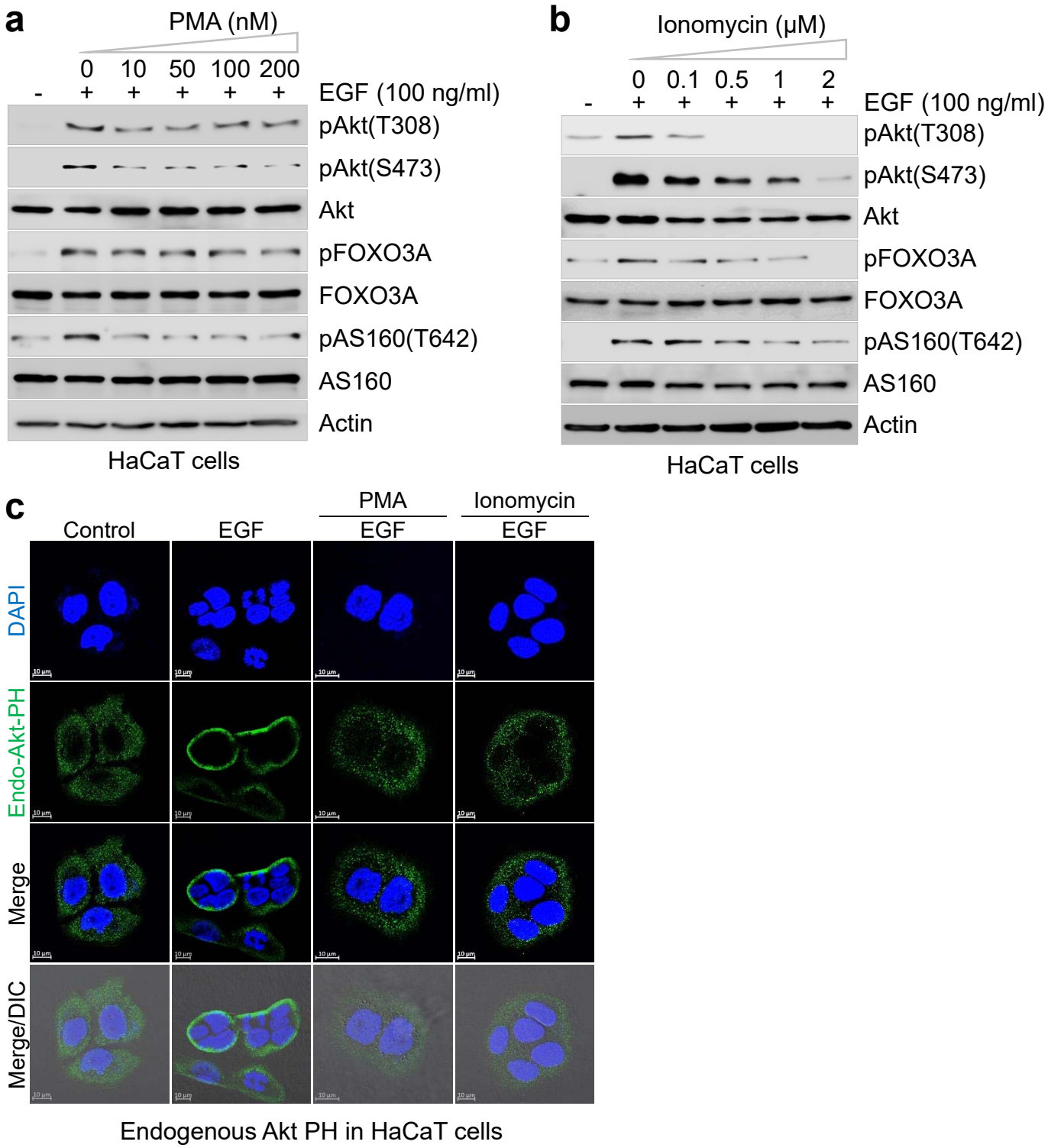

Figure S9. **The effects of higher intracellular Ca^{2+} on EGF signaling and EGF-stimulated membrane localization of endogenous Akt. a**, **b**. Immunoblot analysis of the phosphorylation states of Akt, FOXO3A, and AS160, and the total amounts of the indicated proteins in HaCaT cells. Cells were incubated for 30 min with the indicated concentrations of PMA (**a**) or Ionomycin (**b**), followed by treatment with EGF (100 ng/ml) for 15 min. **c**. Representative fluorescence images of endogenous Akt in HaCaT cells. Cells were serum-starved for 3 h, followed by pretreatment with or without PMA/ionomycin for 30 min before a 15-min stimulation with EGF (100 ng/ml). Cells were stained with anti-Akt PH domain antibody and visualized with FITC-conjugated secondary antibody.